공학석사 학위논문

Intradermal delivery of adipose-derived secretome-loaded liposome via iontophoresis for effective anti-photoaging

이온영동을 이용한

지방 유래 줄기 세포 분비물 담지 리포솜

진피내 전달의 효율적인 광노화 방지 효과

2023년 2월

서울대학교 대학원

화학생물공학부

신 은 혜

Intradermal delivery of adipose-derived secretome- loaded liposome via iontophoresis for effective anti-photoaging

지도 교수 황 석 연

이 논문을 공학석사 학위논문으로 제출함
2023년 2월

서울대학교 대학원
화학생물공학부
신 은 혜

신은혜의 공학석사 학위논문을 인준함
2023년 2월

위 원 장 _____ 이 윤 우 _____ (인)

부위원장 _____ 황 석 연 _____ (인)

위 원 _____ 김 병 수 _____ (인)

초 록

주요어: 지방유래줄기세포, 지방유래줄기세포 분비물, 광노화 효과, 진피내 전달, 이온영동, 파라크린 효과

학 번: 2021-28304

지방 유래 줄기 세포 분비물은 이미 여러 논문을 통해 항광노화 효과가 확인되었다. 하지만 주입을 통한 줄기세포의 전달은 생착이 어려울 뿐만 아니라 줄기 세포 전달 후 암으로의 분화 가능성을 가지기 때문에 좋은 항광노화 효과를 보이면서도 더 안전한 전달 방법을 찾고자 하였다. 이를 위해 본 연구에서는 리포좀과 이온 영동을 사용하여 지방 유래 줄기 세포 분비물을 더 깊이 전달하는 방법을 사용하였다. 이와 같은 진피내 전달 방법을 사용하여 지방 유래 줄기 세포 분비물을 진피층까지 전달했을 때, 수동적으로 전달했을 때보다 더 나은 항광노화 효과를 갖는다는 것을 확인하였다.

*in vitro*에서 지방 유래 줄기 세포 분비물의 항산화 효과를 확인하였다. 또한, PCR을 통해 광노화 관련 상향 조절 유전자가 억제되는 경향과 하향 조절 유전자는 발현이 촉진되는 경향을 확인하였다. 뿐만 아니라 지방 유래 줄기 세포 분비물을 담지한 리포좀 또한 *in vitro*에서 지방 유래 줄기 세포 분비물과 같은 효과를 보였다. 동물 실험을 통해 리포좀과 이온 영동을 통해서 더 깊게 전달된 지방 유래 줄기 세포 분비물이 수동적으로 전달시킨 실험군 보다 자외선으로 인한 염증효과가 더 적게 나타남과 collagen, elastin, hyaluronic acid과 같은 세포외기질의 구성성분의 양이 더 많음을 입증했다.

이로써 지방 유래 줄기 세포 분비물의 광노화 효과는 진피내 전달을 통해 극대화될 수 있음을 확인하였다.

목 차

표 목차

그림 목차

1. Introduction

Skin aging is the phenomenon occurring when the extracellular matrix (ECM) in the dermis diminishes for some reason and accompanies dryness, toughness, and epidermal thickness.[1] There are two main causes of skin aging; intrinsic aging caused by cumulative genetic damage and extrinsic aging caused principally by ultraviolet light (UV), which is photoaging.[2] Photoaging is induced by two types of UV, UVA (315-400 nm) and UVB (280-315 nm), which pass through a dense ozone layer and penetrate the epidermis of the skin.[3] UVB affects mostly the epidermis and causes direct damage to DNA, RNA, and proteins.[4] As UVA has a long wavelength, it can penetrate the epidermis and reach the dermis layer.[5] Moreover, UVA mainly makes reactive oxygen species (ROS), which leads to a photoaging pathway. ROS reduces ECM which includes collagen, elastin, and glycosaminoglycans (GAGs) through increasing matrix metalloproteases (MMPs) synthesis and suppressing ECM synthesis.[6] Therefore, it is essential to alleviate oxidative stress caused by UV to prevent photoaging of the skin.

Adipose-derived stem cells (ADSC) have been widely used in reconstructive and regenerative medicine.[7] Also, they protect skin from ROS damage generated by UV [8] and these therapeutic effects are primarily attributed to antioxidant and paracrine effects.[9] As a stem cell therapy, ADSC has some cell-related challenges including coagulation activation, tumor formation, and immune rejection.[10] It is one of the strategies to overcome these risks to use secreted factors from ADSC which are dried by precipitation with a compressed fluid anti-solvent (PCA) process (ADSC-CM). PCA process uses carbon dioxide (CO_2) to get the dried powder of the solution. ADSC-CM contains bioactive molecules secreted from ADSC and has similar therapeutic effects as ADSC.[11],[12] Herein, to avoid the risk of using ADSC and obtain the anti-photoaging effect of ADSC, I used ADSC-CM, not ADSC in itself

Dermal drug delivery is frequently used as the skin is suitable for the administration of various dermatological drugs.[13] However, due to the function of the skin which provides a protective barrier from hazardous external environments, delivering drugs and proteins into the dermis in a passive way has restrictions. As the ADSC-CM contains proteins such as growth factors including transforming growth factor beta (TGF-β), vascular endothelial growth factor (VEGF), basic fibroblast growth factor (bFGF), and hepatocyte growth factor (HGF), passive delivery of the ADSC-CM shows low efficiency.[14],[15] To surmount difficulties, among the used methods as penetration enhancers, liposomes have been widely used as they have flexibility and ability to penetrate the epidermis of the skin.[16] As a component of liposome, cholesterol can improve the stability of liposomes by preventing liposome aggregation. Furthermore, the biocompatibility of asolectin lipid and cholesterol has been confirmed. For these reasons, I used asolectin lipid and cholesterol to make small, stable, and biocompatible liposomes.

Iontophoresis is one of the physical enhancers for drug delivery through the skin.[17] Because iontophoresis employs a repulsive force between electrons and charged substances to facilitate the mobility of drugs, the battery using reverse electrodialysis (RED) technology was used as an external source to flow current. According to our laboratory's previous works, RED technology-derived iontophoresis showed effective skin penetration of charged liposomes.[18],[19] As a result, I delivered ADSC-CM into the dermis by applying enhancers and observed more effective anti-photoaging effect than passively delivered ADSC-CM.

2. Results

2.1. Characterization of ADSC-CM

UV irradiation acts as a stressor to the cell and generates ROS.[20] ROS causes up-regulation of MMP, lipid oxidation, DNA damage, and protein

damage at a molecular level, which leads to photocarcinogenesis, apoptosis, senescence, and ECM degradation.[21] Especially ECM degradation leads to wrinkles, weakened elasticity, and dryness, which are symptoms of photoaging. Therefore, ROS scavenging ability is a crucial factor as an anti-photoaging material. To assess intracellular ROS levels of human dermal fibroblast (HDF), I used a 2',7'-dichlorofluorescin diacetate (DCFH-DA) assay and measured the intensity of 2', 7' –dichlorofluorescein (DCF), which is the oxidization result of DCFH-DA by ROS (**Figure 1A**). UV was irradiated at 0, 20, 40, 60, 80, and 100 mJ/cm^2 on HDF. With the increase in the dose of UV irradiation, the ROS level of HDF increased in a dose-dependent manner and showed a 49% increase in 100 mJ/cm^2 compared to the non-irradiated group. To investigate the antioxidant effect of ADSC-CM, ADSC-CM was treated in cells after UV irradiation (**Figure 1B**). Compared to the ROS level of the non-irradiated group, the ROS levels in the UV-irradiated group without ADSC-CM increased by 14% and, when 1 mg/mL ADSC-CM was treated after UV radiation, decreased by 22%.

The gene expression levels of hyaluronic acid synthase 1 (HAS1), collagen1 α1 (COL1α1), and matrix metalloproteinases 2 (MMP2) were compared through real-time-quantitative polymerase chain reaction (RT-qPCR) to investigate how the ADSC-CM affects the photoaging-related gene expression. As shown in **Figure 1C**, the mRNA expression level of HAS1 was down-regulated in the UV-irradiated group without ADSC-CM, resulting in 0.88-fold. However, as the concentration of ADSC-CM increased, the mRNA expression level of HAS1 was up-regulated to 4.99-fold in the UV-irradiated group treated with 1 mg/mL ADSC-CM. Regarding COL1α1, like HAS1, the mRNA expression level of COL1α1 decreased in the UV-irradiated group without ADSC-CM, resulting in 0.58-fold. The mRNA expression level of COL1α1 also increased in a dose-dependent manner and reached 2.38-fold in the UV-irradiated group treated with 1 mg/mL ADSC-CM (**Figure 1D**). As for MMP2, the mRNA

expression level showed an increased level, 1.30-fold, in the UV-irradiated group without ADSC-CM (**Figure 1E**). In contrast, as the concentration of ADSC-CM increased, the mRNA expression level of MMP2 declined to a level similar to that of the non-irradiated group, 0.93-fold, at 0.5 mg/mL. The p-value between the non-irradiated group and 0.5 mg/mL ADSC-CM treated group is 0.9997.

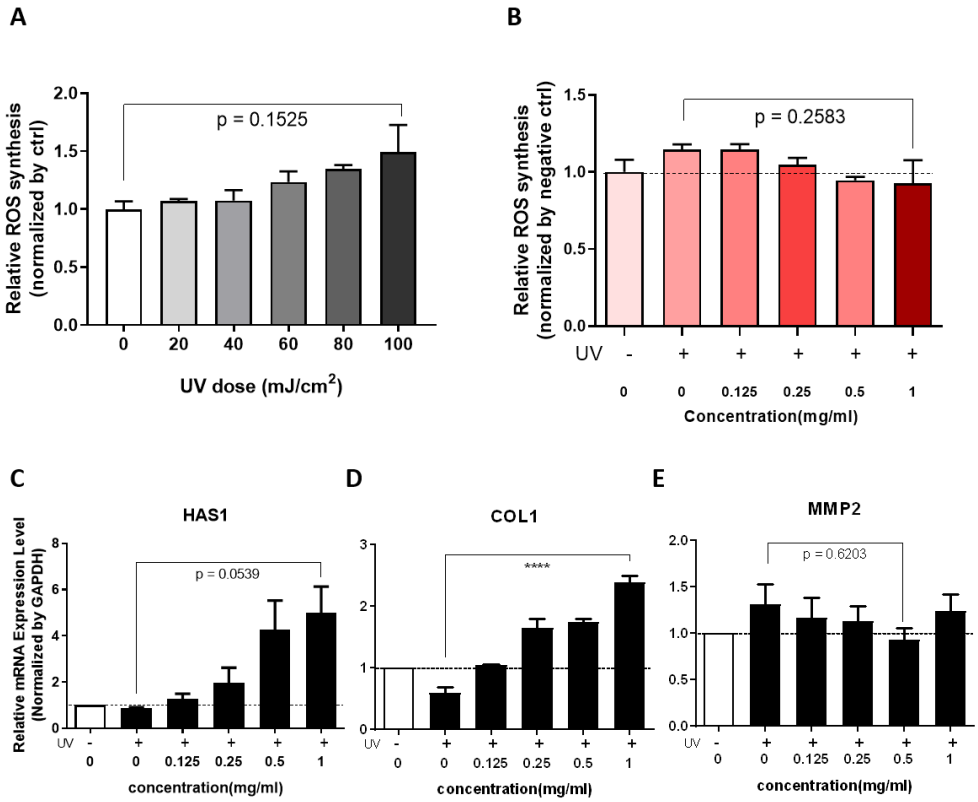

Figure 1 UV-caused ROS and antioxidant effect of ADSC-CM (A) ROS assay was used to measure the ROS level increased by UV. All ROS assays were normalized by the control's fluorescent intensity which represents the amount of ROS. (B) ROS assays were performed to verify the antioxidant effect of ADSC-CM in HDF. (C) RT-qPCR was carried out to HDF to check the change in gene expression according to the increase in the concentration of ADSC-CM after UV irradiation. Statistical significance was calculated by ordinary one-way ANOVA

(*p<0.05; **p<0.01; ***p<0.001; ****p<0.0001; ns)

2.2. Characterization of ADSC-CM encapsulating liposome (CM_Lipo)

I prepared liposomes as a nanocarrier consisting of asolectin lipids and cholesterol to deliver ADSC-CM intradermally (**Figure 2A**). Since repulsive force between charged surfaces prevents liposome aggregation, the stability of a liposome increases with increasing zeta potential. To compare the stability of liposomes with four mass ratios, I measured the zeta potential of liposomes with the asolectin lipids: cholesterol mass ratio of 7:3, 8:2, 9:1, and 10:0 every 7 days for 21 days.[22],[23],[24],[25] The average zeta potential was -26.82 mV at 10:0, -27.58 mV at 9:2, -27.82 mV at 8:2, and -26.58 mV at 7:3 (**Figure 2B).** The liposome of 8:2 composition showed the highest average zeta potential. The average sizes of liposomes with each composition varied, but the optimal size of liposomes was obtained in an 8:2 composition (**Figure 2C)**. As a result, a mass ratio of 8:2, the most stable composition among the four ratios, was chosen for the composition of liposomes.

The sizes and zeta potentials of CM_Lipo were measured (**Figure 2D)**. The average size of CM_Lipo is 126.6 nm, and the average zeta potential is -25.80 mV. It is known that a liposome size under 300 nm can be delivered to the deep layers of the skin to some extent, 126.68 nm sized liposome is small enough to penetrate the epidermis.[26] In addition, the stability of CM_Lipo was also determined by measuring size and zeta potential every 7 days for 3 weeks (**Figure 2E**). Although the size gradually increased from 111.2 nm to 147.8 nm, the size was still small enough to pass through the epidermis in 3 weeks after liposomal formation. The zeta potential had changed from -25.50 mV to -22.35 mV during measurements, which doesn't indicate any significant alterations (the p-value 0.9535).

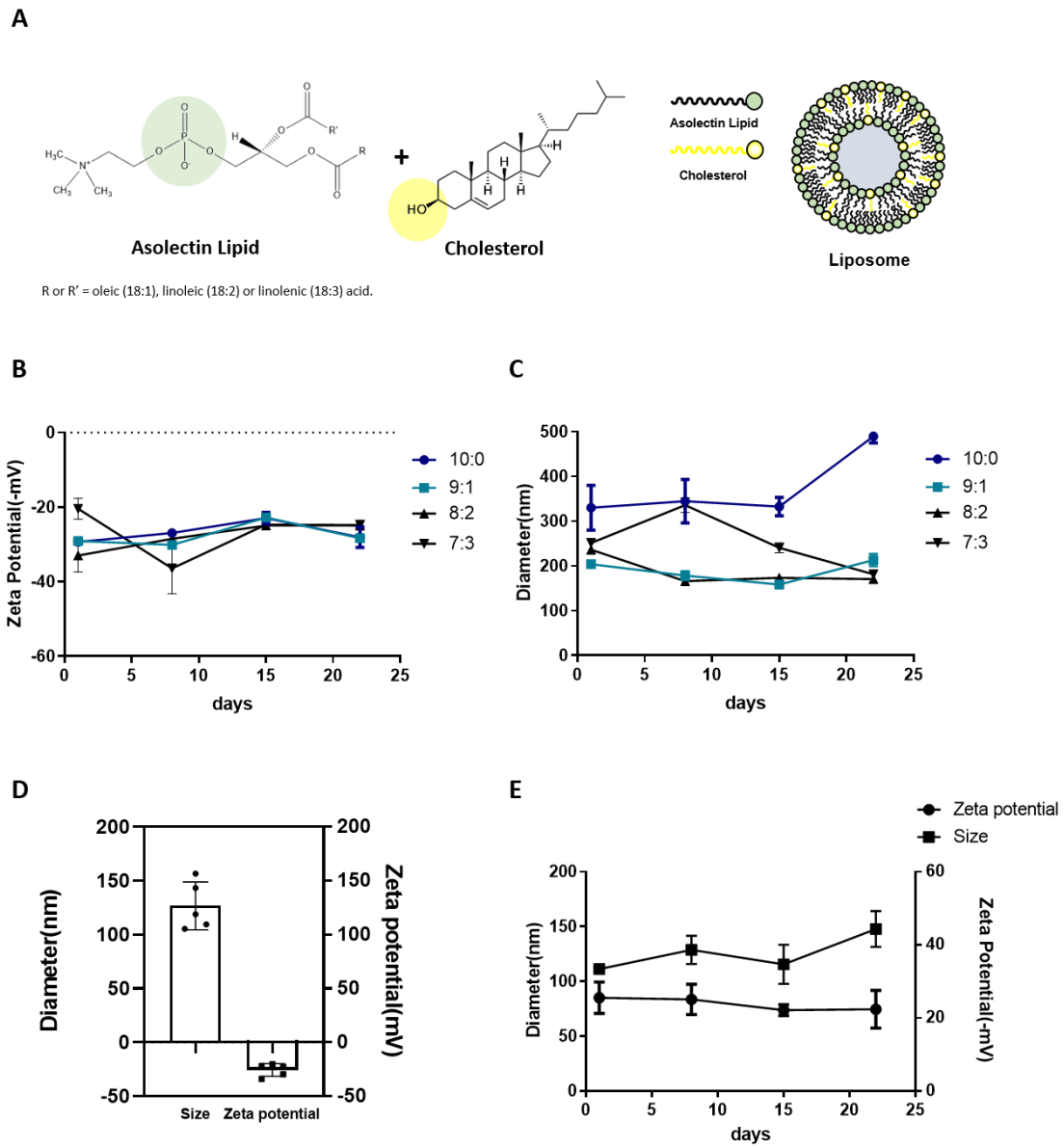

Figure 2 The property of liposome and CM_Lipo (A) The component of liposome and image of liposome we used. The green one represents asolectin lipid. The yellow one represents cholesterol. R or R' = oleic (18:1), linoleic (18:2) or linolenic (18:3) acid. (B) Zeta potentials of liposomes dependent on various mass ratios of components (C) Sizes of liposomes dependent of various mass ratios of components. (D) The average size and zeta potential of CM_Lipo. (E) The changes of size and zeta potential in CM_Lipo for 21days.

To confirm the ROS scavenging ability of CM_Lipo, the ROS assay was performed on HDF (**Figure 3A**). The groups were divided into non-irradiated group and UV-irradiated groups which were treated with or without CM_Lipo (0.02, 0.04, 0.08, 0.2 mg/mL). When the UV was irradiated to HDF without CM_Lipo, the ROS level increased by 7% compared to the non-irradiated group. As the concentration of CM_Lipo increased, ROS levels decreased in a dose-dependent manner and showed a 32% decrease at 0.2 mg/mL compared to the UV-irradiated group without CM_Lipo. In common with the ROS assay of ADSC-CM, UV radiation caused ROS, and delivered CM_Lipo showed an antioxidant effect.

TGF- β is the main factor related to ECM synthesis and MMP synthesis.[27],[28] The ROS caused by UV irradiation reduces the expression of TGF- β and, consequently leads to a decrease in ECM synthesis and an increase in MMP synthesis.[29], [30] To verify the effect of CM_Lipo on the expression of TGF- β via ROS scavenging ability, a TGF-β enzyme-linked immunosorbent assay (ELISA) was conducted. As shown in **Figure 3B**, UV irradiation decreased the protein expression of TGF- β, but when CM_Lipo was treated at 0.2 mg/mL, it recovered to a similar degree to the non-irradiated group (p-value 0.9968).

As shown in **Figure 3C**, the mRNA expression level of HAS1 was down-regulated in the UV-irradiated group without CM_Lipo, resulting in 0.72-fold. As the concentration of CM_Lipo increased, the mRNA expression level of HAS1 was up-regulated to 5.28-fold in the UV-irradiated group with 0.2 mg/mL CM_Lipo. As for COL1α1, the mRNA expression level of COL1α1 was reduced when only UV was irradiated without CM_Lipo, resulting in 0.74-fold. The mRNA expression level of COL1α1 also was enhanced dose-dependently on CM_Lipo, which was up-regulated to 7.13-fold in the UV-irradiated group with 0.2 mg/mL ADSC-CM (**Figure 3D**). The mRNA expression level of MMP2 increased in the UV-irradiated group without CM_Lipo, resulting in 1.85-fold compared to the non-irradiated

control (**Figure 3E**). However, as the concentration of CM_Lipo increased, MMP2 was down-regulated to an mRNA expression level similar to the non-irradiated control at 0.04 mg/mL CM_Lipo (p-value 0.9948).

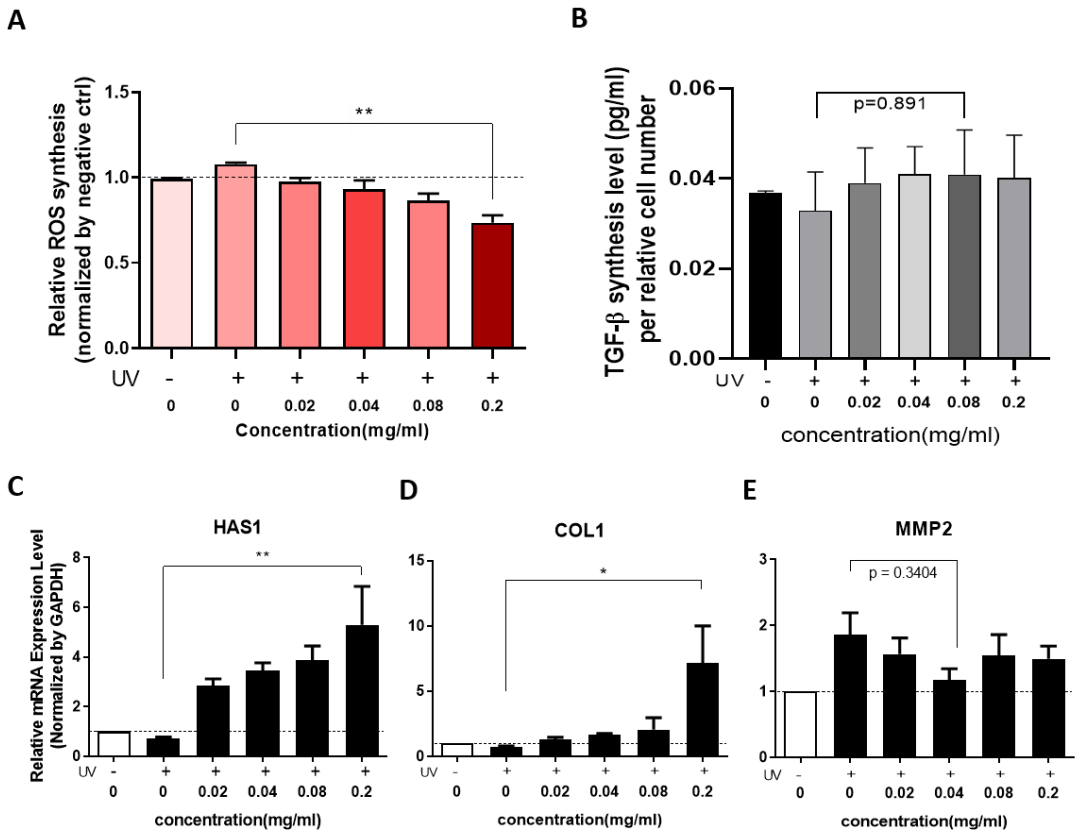

Figure 3 Confirmation of anti-photoaging effect of CM_Lipo (A) ROS asaay with CM_Lipo. All groups were normalized by non-irradiated group's fluorescent intensity in ROS assay. (B) TGF-β ELISA. (C) RT-qPCR showing changes of mRNA expression level in HAS1, COL1 and MMP2.

(*p<0.05; **p<0.01; ***p<0.001; ****p<0.0001)

2.3. Penetration depth of the intradermal delivery system

As I aim to deliver ADSC-CM to the dermis, the penetration depth was measured with a confocal laser scanning microscope (CLSM). As shown in **Figure 4A**, GFP conjugated BSA (B-G) was delivered into the *ex vivo* porcine skin in a passive manner (control) or by being encapsulated in liposome without RED (B-G_Lipo) or with RED (B-G_Lipo+RED). The average penetration depth was 130 μm in the control group and increased by the penetration ability of liposome to 398.33 μm in the B-G_Lipo group. In the B-G_Lipo+RED group, B-G was detected below around 453.75 μm from the surface. Because of the repulsive force between flowing electrons by RED and B-G_Lipo (negative charge), the B-G_Lipo+RED group could show the deepest penetration depth. Since the thicknesses of the epidermis in humans and mice don't exceed 300 μm, proteins delivered by liposome and iontophoresis can reach into the dermis. [31],[32],[33]

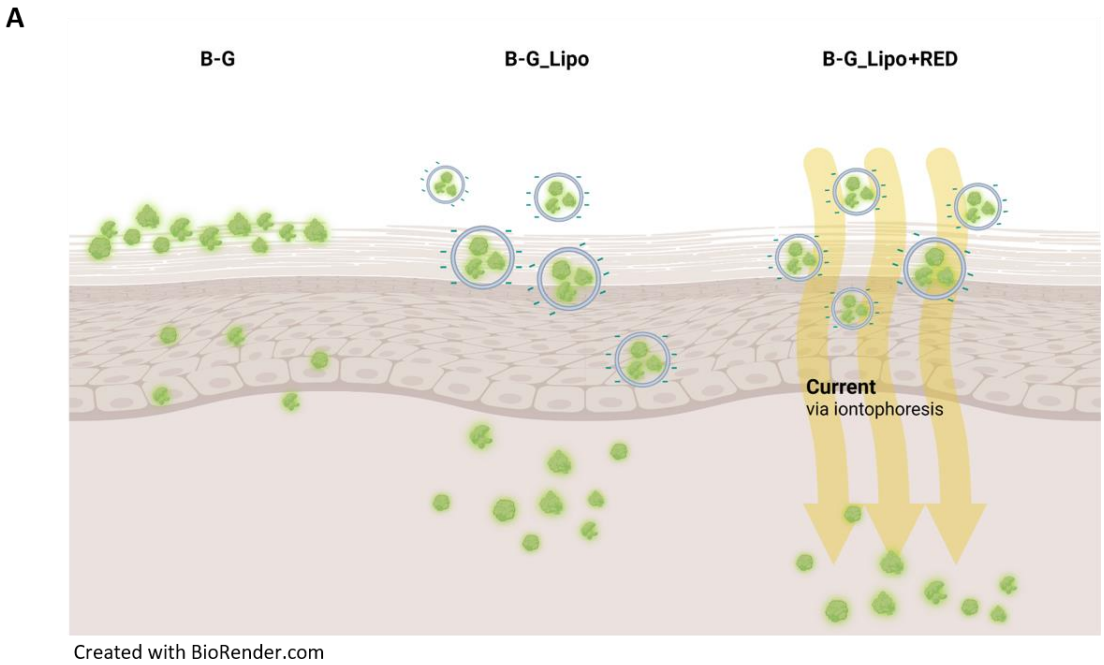

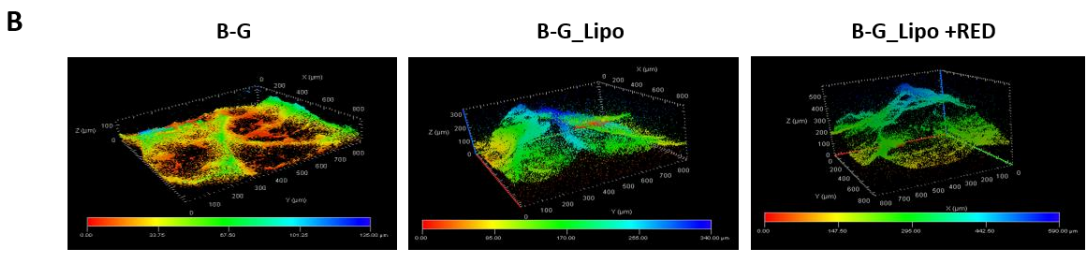

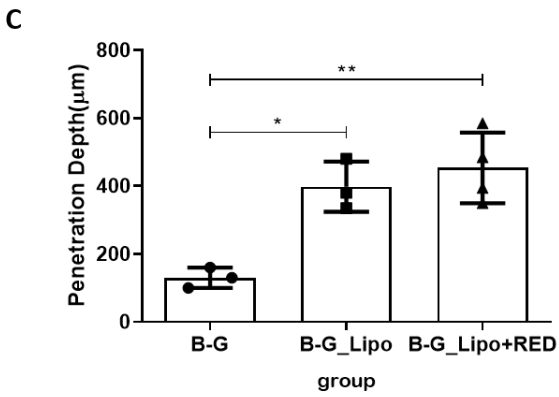

Figure 4 *Ex vivo* experiment for measuring penetration depth of the intradermal delivery system. (A) Scheme of the *ex vivo* experiment. (B) Confocal images showing how deep the BSA-GFP penetrated the porcine skin. (C) Quantification of penetration depth in (B).

(*p<0.05; **p<0.01; ***p<0.001; ****p<0.0001)

2.4. Anti-photoaging effect *in vivo*

An *in vivo* experiment was conducted to check whether ADSC-CM delivered to the dermis layer exhibited a better anti-photoaging effect. To induce wrinkles on BALB/c-nu by UV irradiation, UVA and UVB had been irradiated for 7 weeks with the change of UV dose. The negative control (NC) group was not treated with both UV and ADSC-CM. In the positive control (PC) group, only UV was irradiated. The CM_passive group was applied with a solution containing 50 μg of ADSC-CM for 30 min after UV irradiation, and in the CM_Lipo+RED group, a liposomal solution containing 50 μg of ADSC-CM was delivered using the RED battery for 30 min (**Figure 5**). Images of wrinkles in the dorsal skin of mice were taken using a skin analyzer (**Figure 5A**). UV-induced wrinkles (red arrow) were shown in the PC group and hardly shown in the NC group, CM_Passive, and CM_Lipo+RED group. Through **Figure 5B**, it was possible to visually check whether the photoaging had occurred, and it was observed that the CM_Passive group and CM_Lipo+RED group also had fewer wrinkles than the PC group.

Epidermal thickness is also an indicator of the inflammatory reaction caused by photoaging and is a factor that can be used to determine degrees of photoaging.[34] For quantification of epidermal thickness, the *in vivo* skin tissue was stained with Hematoxylin and Eosin (H&E) and classified into layers of skin tissue (**Figure 5C**). The proportion of epidermis in the NC group increases from 5.99±1.51% to 8.68±1.45% in the PC group. In other words, epidermal thickness (blue arrow) in the PC group is 2.69% thicker than in the NC group. Epidermal thickness decreases to 6.97±1.63% in the CM_Passive group and to 6.25±0.51% in the CM_Lipo+RED group, which is similar to the NC group (p-value 0.9872) (**Figure 6A**).

As shown in **Figure 6B**, the proportion of the dermis showed the opposite tendency in epidermal thickness. Compared to the NC group, the proportion of dermis in the skin was reduced in the PC group from 93.59±2.55% to

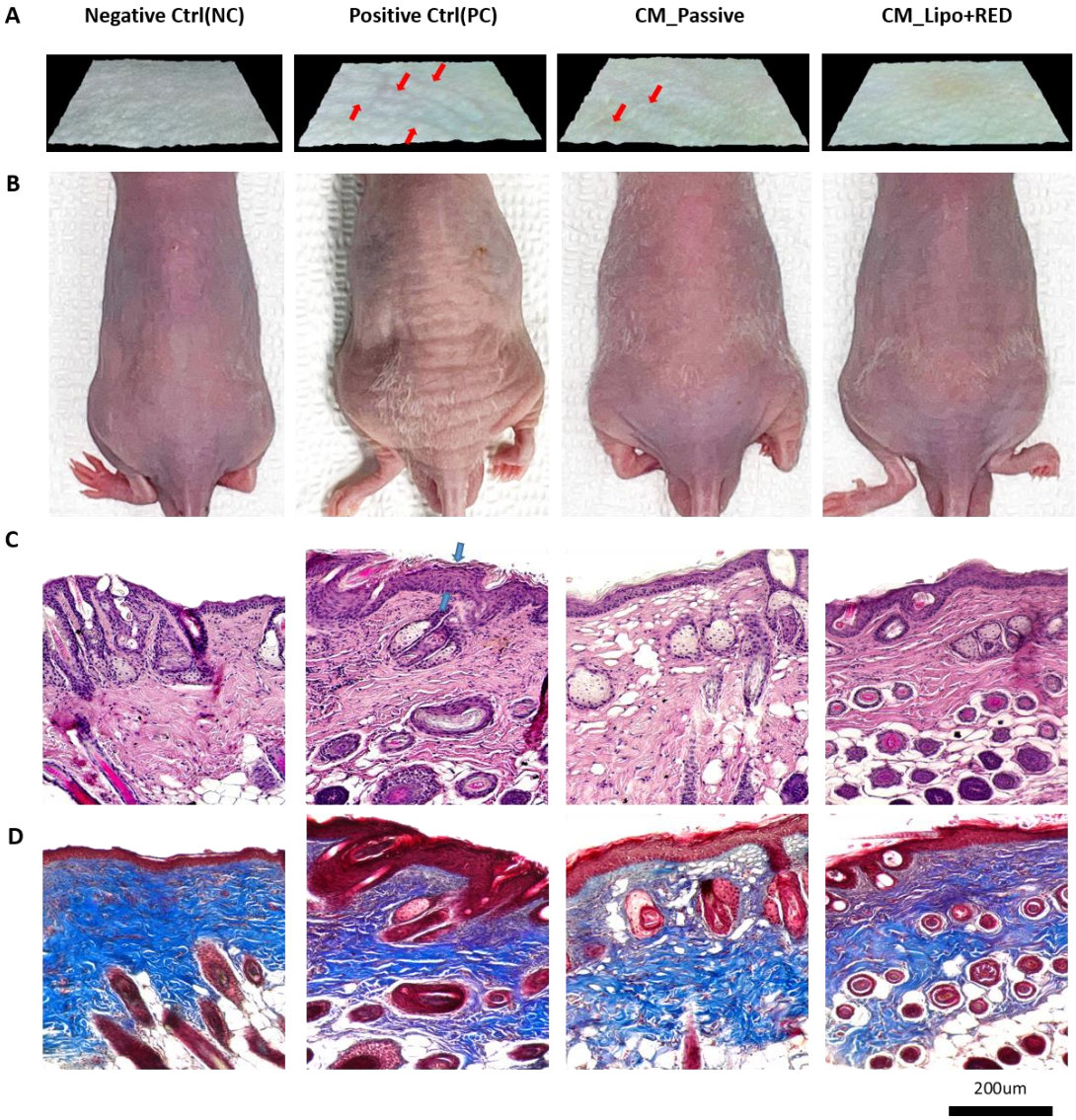

Figure 5 The results of *in vivo* experiment. (A) The images taken by skin analyzer at the end of the experiment. (B) Photographs of BLAB/c-nu mice taken after anesthesia on the last day of the experiment. (C) The H&E staining images of each group. We can see layers of skin through H&E images. (D) The MTC staining images of each group. The amount of collagen can be determined by the blue colored part.

90.46±2.01%. When ADSC-CM was applied passively on the UV-irradiated mice, the proportion of dermis increased to 92.47±0.64% in the CM_Passive group. In the CM_Lipo+RED group, the bigger proportion increase was shown up to 93.32±0.47% than the CM_Passive group. In addition, the intensity of blue in Masson trichrome (MTC) staining was measured per unit area to quantify the collagen density in the dermis layer (**Figure 6B**). The blue intensity in the PC group decreased compared to the NC group from 17089±544 to 14342±1824. This result can be interpreted as a decrease in the total amount of collagen as synthesis was suppressed and breakdown occurred in photoaging. CM_Passive group showed higher collagen density, 17191±758, than the PC group. CM_Lipo+RED group showed higher collagen density, 21257±1089, than the CM_Passive group, which indicates more collagen was synthesized and less collagen was broken down when ADSC-CM is delivered by liposome and RED.

An elastin assay was conducted to validate that elastin degradation is suppressed by ADSC-CM and that more elastin is synthesized because intradermally delivered ADSC-CM can stimulate fibroblasts in the dermis to synthesize elastin more (**Figure 6C**). The amount of elastin in the PC group decreased compared to the NC group from 78.05±8.85 to 72.72 ±12.43 μg/mg. The CM_Passive group showed a similar value, 69.52±1.82 μg/mg, with the PC group (p-value 0.97). In contrast, the CM_Lipo+RED group showed a higher amount of elastin, 87.16±12.52 μg/mg than the NC group beyond the effect of preventing the photoaging effect. This is because the synthesis of elastin was also increased by TGF-β regulation which was previously confirmed *in vitro*. [35]

When UV induces photoaging, expression of hyaluronidase is up-regulated and expression of HAS1 is down-regulated.[36] The amount of HA was measured through an HA assay to evaluate the anti-photoaging effect in terms of HA (**Figure 6D**). Compared to the NC group, the amount of HA decreased in the PC group due to the activation of hyaluronidase and

inhibition of the expression of HAS1. An experimental result in the CM_Lipo+RED group showed more HA than in the CM_Passive group.

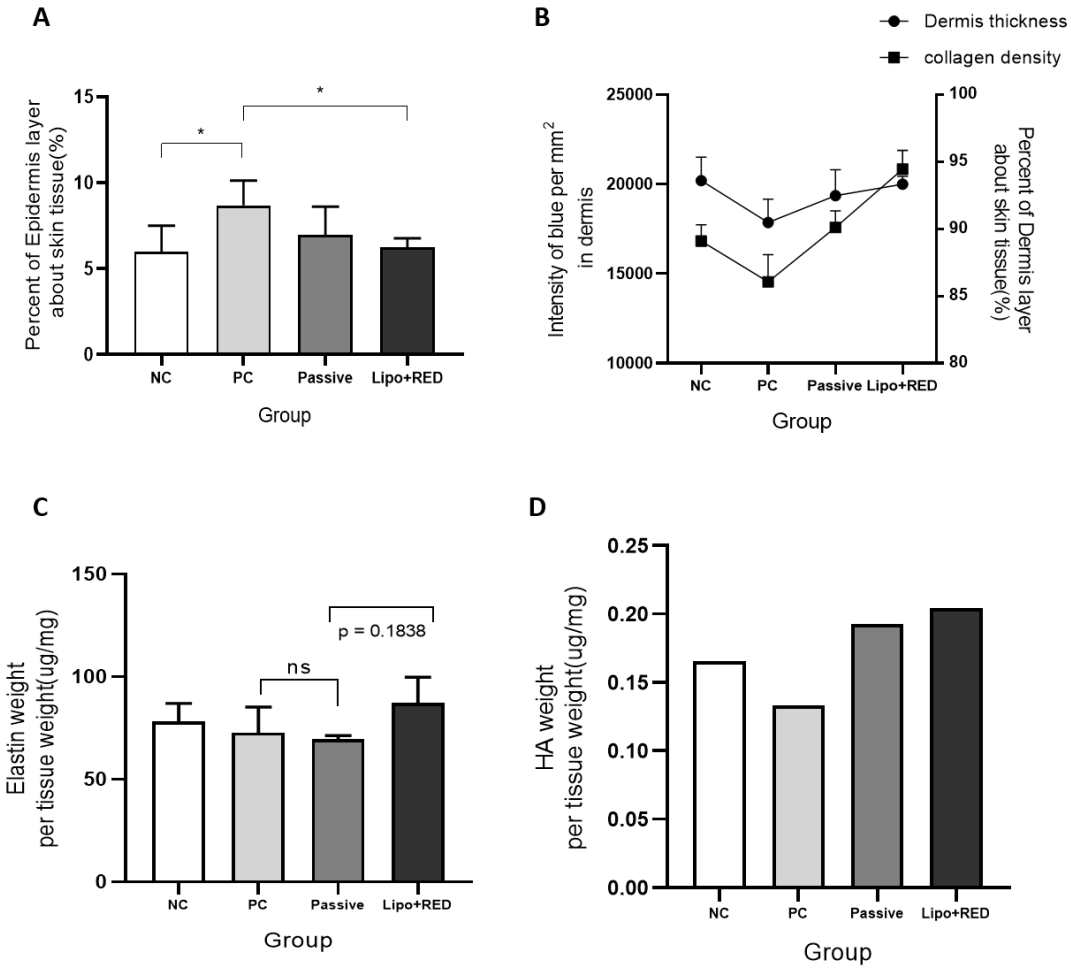

Figure 6 The quantification graph for confirming better anti-photoaging effect in CM_Lipo+IP groups. (A) Epidermal thickness made by calculating epidermis thickness per skin (epidermis + dermis) through H&E images. (B) The change of dermis thickness and collagen density dependent on each group. (C) Elastin assay. The y-axis represents the weight of elastin per skin tissue weight. (D) HA assay. The y-axis represents the weight of HA per skin tissue weight

(*p<0.05; **p<0.01; ***p<0.001; ****p<0.0001)

3. Discussion

UV is the main factor of skin photoaging resulting in wrinkles, dryness, and reduced elasticity of the skin. UV induces ROS, which reduces ECM by increasing MMPs and it is urgent to reduce ROS levels to prevent skin photoaging. As secreted factors of ADSC have anti-photoaging effect, I used them with PCA drying process as a component of alleviating ROS in UV irradiated skin. Furthermore, liposome was used as a carrier of ADSC-CM with RED-driven iontophoresis to efficiently penetrate skin epithelium layer. The results demonstrated that CM_Lipo with RED-driven iontophoresis increased expression levels of HAS1 and COL1 and decreased expression level of MMP2 by scavenging ROS.

Since skin photoaging is mainly induced by ROS, generated by UV irradiation, the antioxidant effect can be an indicator for evaluating the protective effect against photoaging. [9], [21] As shown in **Figure 1** and **Figure 3**, ROS synthesis level was reduced as ADSC-CM and CM_Lipo dose dependently in UV irradiated HDFs. Moreover, increased mRNA expression of HAS1 and COL1, and decreased mRNA expression of MMP2 was observed as ADSC-CM and CM_Lipo added to cells. It is well known that, among the secreted factors from ADSC, TGF-β and GDF11 increase the expression of genes related to ECM production such as HAS1 and COL1α1 via paracrine effect.[37],[38] Also, because all the photoaging phenotypes are induced by UV-caused ROS, ROS scavenging effect of ADSC-CM or CM_Lipo can mitigate the photoaging pathway.

As shown in **Figure 2**, liposome with 8:2 mass ratio of asolectin lipid and cholesterol exhibited good stability among 4 mass ratios. As 8:2 mass ratio of liposome components was chosen, I investigated zeta potential and size of CM_Lipo. Moreover, as shown in **Figure 4**, *ex vivo* experiment was conducted to verify whether iontophoresis is helpful for intradermal delivery. The combination of liposome and RED-driven iontophoresis delivered the encapsulated proteins, B-G, deeper than other groups. When proteins are

delivered deeper in *ex vivo*, the more guaranteed efficiency of delivery *in vivo* is.[39],[40]

I examined the properness of liposome composition, confirmed encapsulation, and observed the ability of RED-driven iontophoresis to enhance intradermal delivery.

As ECM fills the empty space inter fibroblasts in the dermis and maintains the elasticity of the skin, wrinkles occur when ECM is insufficient.[41] Collagen in photoaged skin is declined by decreased TGF-β expression and increased MMP expression, especially MMP2, which are all induced by UV-caused ROS. [42], [43] As shown in **Figure 5**, in the CM_Lipo+RED group *in vivo*, collagen was more synthesized by recovery of TGF- β and less degraded by MMP2. Also, as the paracrine effect of ADSC-CM enhances the synthesis of collagen, collagen can be synthesized more when ADSC-CM exists physically nearby fibroblasts through intradermal delivery.[44] In **Figure 6**, the amounts of collagen and elastin were reduced in the PC group. Furthermore, the highest amounts of collagen and elastin were shown in the CM_Lipo+RED group, which is followed by the CM_Passive group.

As for elastin, UV-caused ROS raises the expression of elastase and lowers the expression of TGF-β whose signaling pathway is related to the synthesis of elastin. Thus, more elastin in the CM_Lipo+RED group than in the PC group is explained by the ROS scavenging effect of intradermal delivered ADSC-CM. As I proved *in vitro*, ADSC-CM induces HDF to express more HAS1, which leads to facilitated HA synthesis *in vivo* when ADSC-CM is delivered near HDF in the dermis. Our data shows that CM_Lipo decreases the UV-caused effect on skin wrinkling and inflammation and has a photoprotective effect.

4. Conclusion

ADSC-CM can cause HDFs to induce an anti-photoaging effect which was

shown *in vitro* through ROS scavenging effect and tendency of photoaging related genes, HAS1, COL1, and MMP2. ADSC-CM is composed of large-size proteins that cannot penetrate the skin, so simply applying it on the skin won't effectively elevate the anti-photoaging effect. To facilitate the anti-photoaging effect, ADSC-CM is administered to the dermis via liposome and RED-driven iontophoresis *in vivo*. In conclusion, the ADSC-CM delivered to the location where the photoaging pathway takes place physically demonstrated a better anti-photoaging effect by accelerating the antioxidant effect and paracrine effect.

5. Experimental Section/Methods

Preparation of dried ADSC-CM

The ADSC was cultured in T175 at 37℃ and CO_2 5%. When the confluence of ADSC in T175 was about 90%, the media of ADSC was replaced with phenol-free and low-glucose DMEM. The conditioned media was collected after 4 days, then concentrated with a centrifugal filter (3kda MWCO, American® Ultra-15 Centrifugal Filter Unit). Concentrated media was mixed in a 1.5:1 mixture of dimethyl sulfoxide (DMSO) and acetone. The solution was sprayed at a rate of 1 mL/min into a CO_2 chamber in which conditions were maintained at 200 bar, 20℃.

Preparation of CM_Lipo

To prepare lipid film, 5 mL chloroform solution containing 8 mg asolectin lipid and 2 mg cholesterol was poured into a 250 mL round bottom flask. Chloroform was evaporated using a rotary evaporator for 1 h at 40℃, resulting in lipid film formation. 50 mL of an ADSC-CM solution with a concentration of 0.5 mg/mL was put in the flask. After that, vortexing was followed for 15 min. To decrease and uniformize the sizes of liposomes, liposome solution passed a microfluidizer (Microfluidizer 110P, Microfluidics International Corporation, US) 10 times at 1360 bar. After

that, dialysis (12-14kDa MWCO) was followed in a beaker with deionized water (DW) for 3 days.

The zeta potentials and sizes of liposomes were measured by dynamic light scattering (DLS) device (Nano ZS90, Malvern Panalytical Ltd., UK). The concentration of ADSC-CM encapsulated in the liposome was calculated via the bicinchoninic acid (BCA) assay.

Cell culture for in vitro experiments

In the cell experiment, HDF with the passage number of 4-10 was used. The media was DMEM/HIGH GLUCOSE (Cytiva, Massachusetts, US) containing 10% FBS (Corning, New York, US) and 1% Penicillin-Streptomycin (Gibco™, Massachusetts, US). The proteolytic material used for subculture was Trypsin-EDTA solution 0.25% (Sigma-Aldrich, State of Missouri, US). The cell culture environment was maintained at 37℃ and CO_2 5%.

Quantification of ROS

The HDF was seeded to a 48-well plate with 20000 cells/well. The next day, UV (100 mJ/cm^2) was irradiated with blank DMEM after washing the well with Dulbecco′s Phosphate Buffered Saline (DPBS) (GW Vitek, Seoul, Republic of Korea). After UV irradiation, media containing ADSC-CM or CM_Lipo was treated. 24 h later, the wells were treated with 5 μM of DCF-DA (Invitrogen™, Massachusetts, US). After 30 min, the fluorescence intensity of the DCF which indicates ROS was read using a microplate reader (Tecan, Tecan Group Ltd., Switzerland) by excitation 485 nm/emission 535 nm.

Quantitative real-time PCR

A total of 6 groups was set to determine the effect of ADSC-CM or CM_Lipo on the mRNA expression. There were negative control, positive control, and experimental groups where UV was irradiated and media containing ADSC-CM or CM_Lipo was treated. The HDF in each group was extracted using TRIzol™ Reagent (Invitrogen™, Massachusetts, US).

The mRNA of the extracted cell was made into cDNA using an oligonucleotide primer (Bioneer, Daejeon, Republic of Korea), and RT-qPCR sampling was analyzed through SYBR Green. The primer sequence is listed in Table 1. [45]

Table 1 sequences of genes used for RT-qPCR

	5'	Sequence 3'
HS COL1α1	Forward	TGACCTCAAGATGTGCCACT
	Reverse	CGAACCAGACATGCCTCTTG
HS MMP2	Forward	GCACCCATTTACACCTACACCAA
	Reverse	AGAGCTCCTGAATGCCCTTGA
HS HAS1	Forward	TGTGTATCCTGCATCAGCGGT
	Reverse	CTGGAGGTGTACTTGGTAGCATAACC

Human TGF-β ELISA

HDF was seeded with 14000 cells/well on a 48-well plate, and the experiment was conducted the next day. UV (100 mJ/cm^2) was irradiated with DPBS filled. DPBS were replaced with media suitable for each group. After 24h, the media was collected and activated using 1N HCl and 1N NaOH. The rest of the method followed the manual of the product ELISA kit, BSKH1021, (Bioss Ltd., Massachusetts, US).

Penetration depth of the intradermal delivery system

Porcine skins obtained from micropig (Micropig Franz Cell Membrane, 4x4x1200, APURES, Pyeongtaek, Republic of Korea) were used for *ex vivo* experiment. The bovine serum albumin (BSA) conjugated with green fluorescent protein (GFP) represents the proteins in *ex vivo* experiment. The penetration depth was measured by confocal laser scanning microscope

(CLSM710, Carl Zeiss, Germany) at the NCIRF of Seoul National University with a magnification of 10x and a resolution of 512x512.

Animal experiment

All animal tests and experimental procedures were approved by the Institutional Animal Care and Use Committee of the Seoul National University (#SNU-220601-1). The mouse model used in animal experiments, a seven-week-old BALB/c-Nu male mouse, was purchased from Gapyeong center, Orient Bio Inc. Animal experiment was conducted at the Animal Center for Pharmaceutical Research of Seoul National University, and the temperature is maintained at 22±2℃ (limit value 18-26℃), humidity is 50±5% (30-70%), and lighting is maintained at 150-300 LUX. UV was irradiated 3 times per week for 7 weeks using a UV lamp (BLX-365 UV Crosslinker, Vilber Lourmat, France). In the experimental group where ADSC-CM or CM-Lipo was applied, a solution containing 50 μg of ADSC-CM was treated for each treatment for 30 min and the solution was prevented from flowing using the silicon ring. Skin wrinkles were estimated by a skin analyzer (ds vivo CND-O2R-A, CHOWIS, Republic of Korea) on the last day of the experiment. The dorsal skin of the mouse was harvested the day after the last treatment in week 7, and the skin tissue was stored at –80℃ until each analysis progressed.

H&E staining was performed on *in vivo* experimental skin sections. MTC staining was performed according to conventional methods. The epidermis and dermis thickness were obtained by H&E staining images. Collagen density is obtained by measuring the blue intensity in the MTC staining images (software Image J).

Quantification of elastin

After the *in vivo* experiment, skin tissues were weighed into 10-20 mg for elastin assay. I used Fastin™ - Elastin ASSAY kit (Biocolor Ltd, Newtownabbey, UK) for elastin assay and followed the product guide. As an HA assay, elastin weight varies depending on the tissue weight, so the

weight of the extracted elastin was calculated and normalized by the tissue weight.

Quantification of HA

The amount of HA was measured for checking the activity of HAS1 and suppression of hyaluronidase. The Purple-Jelly Hyaluronic Acid Assay kit (Biocolor Ltd., Newtownabbey, UK) was used to confirm a change of HA. HA was extracted from 50±10 mg tissues of each group and analyzed according to the product guide. The amount of HA varies depending on the weight of the extracted skin, so the mass of HA was calculated for each group and normalized by the mass of the tissue.

Data analysis

Data were expressed as mean±standard deviation and were analyzed using one-way analysis of variance (ANOVA) for multiple comparisons. p-values less than 0.05 are considered statistically significant. In some occasions, even though the p-value is greater than 0.05, a tendency is considered significant.

참고 문헌

[1] S. Chen, Z. He, J. Xu, *Stem Cell Research & Therapy* **2020**, *11* (1), 1.

[2] D. J. Tobin, *Journal of tissue viability* **2017**, *26* (1), 37.

[3] I. Sjerobabski Masnec, S. Poduje, *Collegium antropologicum* **2008**, *32* (2), 177.

[4] K. J. Gromkowska‐Kępka, A. Puścion‐Jakubik, R. Markiewicz‐Żukowska, K. Socha, *Journal of Cosmetic Dermatology* **2021**, *20* (11), 3427.

[5] J. Krutmann, M. Berneburg, *Der Hautarzt; Zeitschrift fur Dermatologie, Venerologie, und Verwandte Gebiete* **2020**.

[6] X. Chen, C. Yang, G. Jiang, *Advances in Dermatology and Allergology/Postępy Dermatologii i Alergologii* **2021**, *38* (6), 931.

[7] P. Bora, A. S. Majumdar, *Stem cell research & therapy* **2017**, *8* (1), 1.

[8] J. H. Jeong, Y. Fan, G. Y. You, T. H. Choi, S. Kim, *Journal of Plastic, Reconstructive & Aesthetic Surgery* **2015**, *68* (3), 372.

[9] P. Xu, Y. Xin, Z. Zhang, X. Zou, K. Xue, H. Zhang, W. Zhang, K. Liu, *Stem Cell Research & Therapy* **2020**, *11* (1), 1.

[10] O. Y. Bang, E. H. Kim, J. M. Cha, G. J. Moon, *Journal of stroke* **2016**, *18* (3), 256.

[11] R. C. Lai, S. S. Tan, B. J. Teh, S. K. Sze, F. Arslan, D. P. De Kleijn, A. Choo, S. K. Lim, *International journal of proteomics* **2012**, *2012*.

[12] H. Xin, Y. Li, Y. Cui, J. J. Yang, Z. G. Zhang, M. Chopp, *Journal of Cerebral Blood Flow & Metabolism* **2013**, *33* (11), 1711.

[13] F. Sabbagh, B. S. Kim, *Journal of Controlled Release* **2022**, *341*, 132.

[14] Y. Cai, J. Li, C. Jia, Y. He, C. Deng, *Stem Cell Research & Therapy* **2020**, *11* (1), 1.

[15] C. A. Lipinski, F. Lombardo, B. W. Dominy, P. J. Feeney, *Advanced drug delivery reviews* **1997**, *23* (1-3), 3.

[16] M. Ashtikar, K. Nagarsekar, A. Fahr, *Journal of Controlled Release* **2016**, *242*, 126.

[17] W. Turrell, *Proceedings of the Royal Society of Medicine* **1921**, *14* (Electro_Ther), 41.

[18] R. R. Burnette, D. Marrero, *Journal of pharmaceutical sciences* **1986**, *75* (8), 738.

[19] Y.-H. An, J. Lee, D. U. Son, D. H. Kang, M. J. Park, K. W. Cho, S. Kim, S.-H. Kim, J. Ko, M.-H. Jang, *ACS nano* **2020**, *14* (4), 4523.

[20] C. S. Sander, H. Chang, F. Hamm, P. Elsner, J. J. Thiele, *International journal of dermatology* **2004**, *43* (5), 326.

[21] K. Scharffetter-Kochanek, J. Wenk, P. Brenneisen, R. Blaudschun, M. Wlaschek, in Springer, **1997**.

[22] D. Giron, J. Swarbrick, Encyclopedia of Pharmaceutical Science and Technology. Swarbrick, J., eds: **2013**.
[23] S. Samimi, N. Maghsoudnia, R. B. Eftekhari, F. Dorkoosh, *Characterization and biology of nanomaterials for drug delivery* **2019**, 47.
[24] S. Honary, F. Zahir, *Tropical journal of pharmaceutical research* **2013**, *12* (2), 265.
[25] S. Das, A. Chaudhury, *Aaps Pharmscitech* **2011**, *12* (1), 62.
[26] D. D. Verma, S. Verma, G. Blume, A. Fahr, *International journal of pharmaceutics* **2003**, *258* (1-2), 141.
[27] A. M. B. S. M. Roberts, *Kidney Int* **1992**, *41*, 557.
[28] C.-R. Kim, Y.-M. Kim, M.-K. Lee, I.-H. Kim, Y.-H. Choi, T.-J. Nam, *International Journal of Molecular Medicine* **2017**, *39* (1), 31.
[29] G. Yang, Y. Li, E. K. Nishimura, H. Xin, A. Zhou, Y. Guo, L. Dong, M. F. Denning, B. J. Nickoloff, R. Cui, *Molecular cell* **2008**, *32* (4), 554.
[30] J. Zussman, J. Ahdout, J. Kim, *Journal of the American Academy of Dermatology* **2010**, *63* (3), 507.
[31] J. Sandby-Moller, T. Poulsen, H. C. Wulf, *Acta Dermato Venereologica* **2003**, *83* (6), 410.
[32] P. Oltulu, B. Ince, N. Kokbudak, S. Findik, F. Kilinc, *Turkish Journal of Plastic Surgery* **2018**, *26* (2), 56.
[33] J. E. Gudjonsson, A. Johnston, M. Dyson, H. Valdimarsson, J. T. Elder, *Journal of Investigative Dermatology* **2007**, *127* (6), 1292.
[34] X. Li, T. Matsumoto, M. Takuwa, M. Saeed Ebrahim Shaiku Ali, T. Hirabashi, H. Kondo, H. Fujino, *Biomedicines* **2020**, *8* (2), 18.
[35] V. Kähäri, D. Olsen, R. Rhudy, P. Carrillo, Y. Chen, J. Uitto, *Laboratory investigation; a journal of technical methods and pathology* **1992**, *66* (5), 580.
[36] K. Madan, S. Nanda, *Bioorganic Chemistry* **2018**, *77*, 159.
[37] H. Jung, H. H. Kim, D. H. Lee, Y.-S. Hwang, H.-C. Yang, J.-C. Park, *Cytotechnology* **2011**, *63*, 57.
[38] L. Mazini, L. Rochette, G. Malka, *Regen. Med* **2020**.
[39] N. Döge, *Evaluation of ex vivo human skin as model for the investigation of nanoparticle-based drug delivery systems for anti-inflammatory topical dermatotherapy*, Freie Universitaet Berlin (Germany), **2018**.
[40] Y. Fan, Y. Lu, B. Cheng, Y. Wei, Y. Wei, J. Piao, F. Li, H. Zheng, *International Journal of Pharmaceutics* **2022**, *621*, 121789.
[41] M. C. McCabe, R. C. Hill, K. Calderone, Y. Cui, Y. Yan, T. Quan, G. J. Fisher, K. C. Hansen, *Matrix biology plus* **2020**, *8*, 100041.
[42] M. Toth, A. Sohail, R. Fridman, in Springer, **2012**.
[43] R. T. Aimes, J. P. Quigley, *Journal of Biological Chemistry* **1995**, *270* (11), 5872.
[44] H. Jung, H. H. Kim, D. H. Lee, Y.-S. Hwang, H.-C. Yang, J.-C. Park, *Cytotechnology* **2011**, *63* (1), 57.

[45] T. Wang, S. Guo, X. Liu, N. Xv, S. Zhang, *International journal of clinical and experimental pathology* **2015**, *8* (12), 15739.

Abstract

외국어 제목

Shin Eunhye
School of Chemical and Biological Engineering
The Graduate School
Seoul National University

Keywords: ADSC-CM, Anti-photoaging, Intradermal delivery, ROS, Liposome, PCA process
Student Number: 2021-28304

Recently, it has been reported that secreted factors from adipose-derived stem cells (ADSC) have an anti-photoaging effect. The secreted factors stimulate fibroblasts to induce an antioxidant effect and paracrine effects, which leads to anti-photoaging. In this study, I dried ADSC culture media containing secreted factors with a compressed fluid anti-solvent process (ADSC-CM) and encapsulated ADSC-CM into nanocarrier liposome to elevate the anti-photoaging effect *in vivo*. When the ADSC-CM solution was treated to ultraviolet light (UV)-damaged cells, the expressions of HAS1 and COL1 were up-regulated and the expression of MMP2 was down-regulated *in vitro*. To enhance delivery efficiency, ADSC-CM was encapsulated in the biocompatible liposome (CM_Lipo). Treating CM_Lipo to UV-damaged cells induced the mRNA expressions of HAS1, COL1, and MMP2 which are consistent with the mRNA expressions of ADSC-CM-treated cells. Furthermore, in *ex vivo* porcine skin, a higher delivery efficiency than passive delivery was observed when a liposome and reverse electrodialysis (RED) – driven iontophoresis was applied to delivery. In the UV-induced wrinkling model, intradermal delivered CM_Lipo alleviated photoaging of the skin. Overall, I achieved qualitative delivery of ADSC-CM and verified that ADSC-CM effectively mitigates the photoaging when located nearby UV-damaged cells.